Separation and Purification Technology 371 (2025) 133261

Contents lists available at ScienceDirect

Separation and Purification Technology

journal homepage: www.elsevier.com/locate/seppur

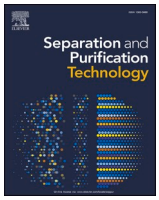

Binary mixtures of menthol and alkanoic acids as green solvents for efficient astaxanthin recovery from *Aristaeomorpha foliacea* shrimp shells

Federica Mancarella [a], Francesco Milano [b], Paola Semeraro [a,1], Vincenzo De Leo [c], Francesco Messa [a], Serena Perrone [a], Antonio Salomone [c], Miriana Durante [b], Marcello Salvatore Lenucci [a], Maria De Benedictis [b], Angelo Santino [b], Livia Giotta [a,d,*], Ludovico Valli [a,d]

[a] *Dipartimento di Scienze e Tecnologie Biologiche e Ambientali, Università del Salento, S.P. Lecce-Monteroni, I-73100 Lecce, Italy*
[b] *Istituto di Scienze delle Produzioni Alimentari (ISPA), Consiglio Nazionale delle Ricerche (CNR), UOS Lecce, S.P. Lecce-Monteroni, I-73100 Lecce, Italy*
[c] *Dipartimento di Chimica, Università degli Studi di Bari "Aldo Moro", Bari, Italy*
[d] *Consorzio Interuniversitario Nazionale per la Scienza e Tecnologia dei Materiali (INSTM), Unità di Lecce, Lecce, Italy*

ARTICLE INFO

Handling editor: B. Van der Bruggen

Keywords:
Seafood industry waste
Eutectic solvents
Xanthophylls
Emulsions
α-cyclodextrin

ABSTRACT

The seafood industry generates large volumes of waste, responsible for serious environmental hazards and high disposal costs. Bioconversion and biorefinery approaches offer effective management of seafood waste, preserving valuable nutrients and supporting sustainable seafood production. Shrimp shells are a rich source of polyunsaturated fatty acids and carotenoids, mainly astaxanthin (AST), whose recovery by means of green strategies represents a challenging goal. In this work, the potential of equimolar binary mixtures of menthol and alkanoic acids (ME:AA) as green solvents for AST recovery from shells of *Aristaeomorpha foliacea* (Risso, 1827) shrimp has been explored, by evaluating both the yield and the stability of the extracted carotenoid. All tested ME:AA exhibited high efficiency for fast AST extraction in mild conditions, while the mixtures containing acetic (ME:C2) and decanoic (ME:C10) acids ensured the maximum stability of the pigment. HPLC analysis highlighted a variety of extracted AST derivatives, mainly consisting of mono- and diesters of fatty acids with variable side chains. Their overall amount allowed to identify mediterranean *A. foliacea* as a shrimp species particularly capable of AST uptake and storage. ATR-FTIR measurements pointed out partial deprotonation of the alkanoic acid component following the extraction process, in agreement with the alkalinity of the $CaCO_3$-rich matrix. Interestingly, the antioxidant capacity of the extracts exceeded the predicted one, based on the AST content, suggesting the co-extraction of additional antioxidant compounds. Finally, α-cyclodextrin was successfully employed as emulsifying agent to prepare stable ME:C10-in-water microemulsions, which drastically enhanced the chemical stability of extracted AST under standard environmental conditions.

1. Introduction

Current methods for management and disposal of waste/by-products produced by the food processing industry are poorly sustainable and often cause environmental concerns. The fishing industry is one of the most impacting sectors due to the increase of global fish demand and the constant growth of aquaculture production. Processing of fish products has generated in recent decades the increase of by-products, composed of heads, viscera, flesh portions, skin, bones, fins, shells and scales, which represent about 70 % of processed species [1,2] and are responsible for significant environmental impact and high disposal costs. However, the parts of marine organisms commonly discarded are a nutritionally important source of high-value bio-compounds such as minerals, lipids, omega-3 polyunsaturated fatty acids, amino acids, collagen, peptides, chitin, enzymes, antioxidant substances and other bioactive molecules suitable for biotechnological, pharmaceutical, nutraceutical and cosmetic applications [2–4]. Therefore, to avoid substantial loss of valuable compounds, better management strategies of

* Corresponding author.
E-mail address: livia.giotta@unisalento.it (L. Giotta).
[1] Present address: Istituto di Scienze dell'Atmosfera e del Clima (ISAC), Consiglio Nazionale delle Ricerche (CNR), UOS Lecce, S.P. Lecce-Monteroni, I-73100 Lecce, Italy.

https://doi.org/10.1016/j.seppur.2025.133261
Received 1 March 2025; Received in revised form 21 April 2025; Accepted 26 April 2025
Available online 28 April 2025

fish by-products are a key point for the transition from a linear to a circular economy model.

Within this context, the recovery of astaxanthin (AST), a carotenoid abundantly present in crustacean by-products, such as shrimp, crawfish, crab, and lobster shells [5], is an excellent opportunity for valorisation of such residues with new, safe, and cost-effective methodologies. AST (3,3′-dihydroxy-β,β'-carotene-4,4′-dione, Fig. 1A) is a reddish-orange xanthophyll occurring in marine and aquatic organisms in its free or esterified forms. In particular, in crustacean by-products AST occurs mainly in form of mono- and diesters of fatty acids [6,7], which are less susceptible to degradation processes, induced by high temperature, oxygen or light, than unesterified astaxanthin [7]. In addition, AST exists in nature predominantly as a mixture of (all-*E*)-isomers composed of two enantiomers (3R,3′R- and 3S,3′S-AST) and a meso compound (3R,3′S-AST), which, at high temperatures and under light and oxidative conditions, can isomerize to Z configurations [8]. AST shows high antioxidant activity [4,5,9] due to its capability to convert free radicals into more stable products [8], reducing the oxidative stress and consequently most of the age-related diseases such as atherosclerosis, metabolic syndrome, osteoporosis, cancer, inflammatory arthritis, or dementia [10,11]. Natural extracts with a high AST content represent therefore a valuable secondary raw material for cosmetic, pharmaceutical or food industries.

Numerous studies reported the extraction of AST from shrimp processing waste using different organic solvents such as acetone, isopropyl alcohol, methanol, hexane, ethyl acetate, ethyl methyl ketone, chloroform, petroleum ether or a combination of them [4,12]. However, conventional extraction methods with these common organic solvents often present important disadvantages including their impact on human health and environment, low extraction yield and loss of bioactivity of extracted compounds [4,13]. A more sustainable approach to recover AST from crustaceans is the use of vegetable oils that offer good extraction yields, great advantage in terms of safety and reduction of carotenoids oxidation processes [14,15]. Nevertheless, the composition of vegetable oils is complex and highly variable, depending on their origin, quality, and production methods, leading to high variability of extraction efficiencies [16]. Moreover, vegetable oils present high viscosities resulting in low effective diffusivity, longer extraction times and higher energy inputs to ensure the proper mixing of the blend [17]. Usually, the extraction of carotenoids by oils is performed at high temperatures to decrease their viscosity and improve the solvent flow through the solid matrices. High temperature procedures present however the drawback to favor the decomposition of thermolabile compounds [13].

To overcome the above-mentioned limitations of conventional solvents of petrochemical origin and vegetable oils, eutectic solvents and deep eutectic solvents (DESs) [18] represent a valid, green and sustainable alternative for marine biomass processing. The suitable and targeted selection of their components might indeed confer low toxicity, environmental friendliness, low cost, easy manufacturing and good biodegradability [19]. DESs are an emerging class of solvents composed of mixtures of two or more hydrogen bond acceptor (HBA) compounds, such as quaternary ammonium salts, and hydrogen bond donor (HBD) compounds, consisting of organic molecular components such as urea, carboxylic acids, polyols or amides, linked by intermolecular interactions, as van der Waals interactions, hydrogen and/or ionic bonds [20]. These compounds, mixed at a specific molar ratio, produce a liquid phase with a melting point much lower than that one predicted based on an ideal behavior. On the other hand, a melting point lower than that one of each individual components in absence of negative deviations from ideality indicates a eutectic mixture, rather than a DES [21]. Most DESs, composed at least of one ionic species, are generally characterized by hydrophilic properties and are classified as type I-IV according to currently accepted nomenclature [22].

The design of new hydrophobic eutectic mixtures based on non-ionic substances, classified as type V DESs [23], has received particular attention in last years. Terpenes have been described as good HBA components to prepare sustainable, cheap and hydrophobic eutectic

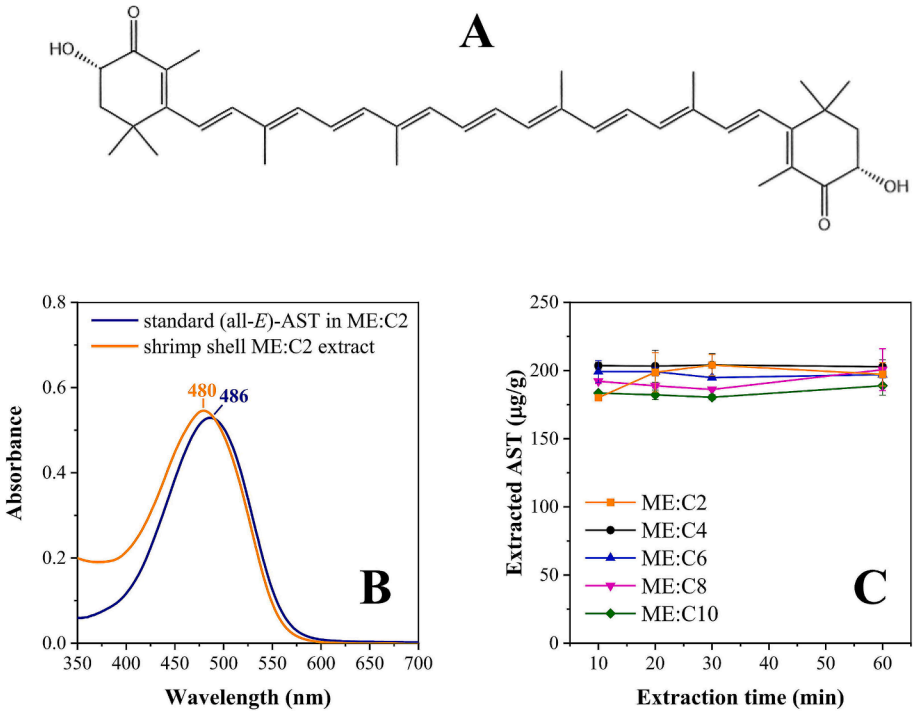

Fig. 1. **A**: Structure of all(*E*)-AST in the free (di-alcoholic) form. **B**: UV–Vis absorption spectra of a 5 µM solution of synthetic all(*E*)-AST in ME:C2 (blue trace) and of a shrimp shell extract, diluted 5 times, obtained using the same solvent (orange trace). **C**: Extracted amounts of AST (as µg of free AST per gram of shrimp shell powder) as a function of extraction time and for different ME:C2n (n = 1–5) solvents. (For interpretation of the references to color in this figure legend, the reader is referred to the web version of this article.)

mixtures to recover astaxanthin and other natural compounds from marine wastes [19]. In recent studies, the good solvent properties of various binary mixtures obtained from the combination of terpenes, as HBA, and carboxylic acids, as HBD, [24,25] were also demonstrated. The monoterpene menthol (ME), obtained from natural resources, is a good candidate to prepare hydrophobic solvent mixtures due to its very low solubility in water. Martins et al. [25] pointed out that the solid–liquid equilibrium (SLE) phase diagrams of mixtures composed of ME and selected long-chain monocarboxylic acids, do not exhibit negative deviations from thermodynamic ideality large enough to induce a significant eutectic point depression and thus cannot be properly classified as DESs. However, several mixtures of ME and carboxylic acids, which are liquid at room temperature in a wide interval of HBD/HBA stoichiometric ratios, are often described as hydrophobic DESs or natural DESs (NADES) in the current literature [26–30], independently on the availability of relevant SLE diagrams highlighting deviations from ideality. Analogously, binary mixtures composed of ME and liquid carboxylic acids are currently labelled as DESs [24,31,32], although they are used at operating temperatures higher than the melting point of the HBD component and thus, in principle, could not even be considered eutectic mixtures. These inconsistencies point out the urgency for a stricter definition of DES and a desirable uniformity of literature designations.

Leaving aside these terminology issues, the mixtures of ME with carboxylic acids appear promising for AST recovery due to their low viscosity [24,33], high hydrophobicity and the acidic character of the HBD moiety. As reported by Villalobos-Castillejos et al. [34], the highest stability of a water-dispersed AST oleoresin was indeed observed at pH 4, thus suggesting the suitability of organic acids as components of solvent mixtures not only for AST extraction yield maximization, but also for shelf-life enhancement purposes.

Hence, in the present research, a series of hydrophobic binary mixtures based on ME and different alkanoic acids (AAs) with variable alkyl chain lengths are proposed as environmentally friendly solvents for the extraction of AST from shells of the Mediterranean red shrimps *Aristaeomorpha foliacea* (Risso, 1827). Specifically, five different combinations, obtained mixing ME and monocarboxylic acids with an even number of carbon atoms varying from 2 to 10, were prepared and tested for their ability to recover AST from the shrimp waste matrix. For the reasons stated above, these mixtures are not referred as DESs in this manuscript, although the current literature often uses this classification for them. Moreover, the label “eutectic” has been used only for the mixture containing decanoic acid, since this is the sole carboxylic acid that is solid at room temperature.

The stability of extracted AST in menthol/alkanoic acid (ME:AA) mixtures was also assessed with the aim to identify the combinations best performing in terms of extraction efficiency and pigment protection from degradative processes. Further information on the chemical composition of extracts was gained by means of high-pressure liquid chromatography (HPLC) and Fourier transform infrared (FTIR) spectroscopy analyses, while a standard decolorization assay was carried out to assess their antioxidant capacity.

Unlike hydrophilic eutectic solvents which can dissolve in water causing in most cases the precipitation, i.e. the separation, of extracted substances by the so-called anti-solvent method [35], hydrophobic eutectic mixtures are immiscible with water and very hard to be separated from solubilized compounds [36,37]. Nevertheless, the natural origin and the well-established biological activity of both ME and the carboxylic acids adopted in this work [38–40] suggest the direct employment of the entire ME:AA extracts as ingredients of specific formulations. Previous investigations have indeed demonstrated that terpene-based eutectic mixtures have the potential to inhibit proliferation of colorectal cancer cells as well as Gram-positive and Gram-negative bacteria [30]. The authors conducted cytotoxicity and anti-proliferative activity tests in the presence of fetal serum albumin, which realistically promoted the dispersion of target hydrophobic samples. With the aim to develop astaxanthin-rich formulations intrinsically biodeliverable and, in addition, physically and chemically stable, we have explored the possibility to achieve the dispersion of ME:AA mixtures and relevant shrimp extracts in aqueous environment by using cyclodextrins (CDs) as complexing agents. CDs are a well-known family of cyclic oligosaccharides able not only to form stable supramolecular complexes with hydrophobic species [41], but also to preserve the encapsulated molecules from degradation processes [42]. CDs can stabilize oil-in-water emulsions forming microcrystals of CD-oil inclusion complexes [43,44]. Moreover, recent investigations have shown that they can be successfully employed to prepare supramolecular DESs, acting as a vehicle for the delivery of poorly soluble drugs [45]. Inspired by these previous outcomes, we used α-cyclodextrin (α-CD), composed of six D-glucopyranose units linked by α-(1–4) bonds, as an emulsifying agent to prepare stable ME:AA-in-water emulsions, which were characterized not only for their physical stability, chemical composition, and microscopic structure, but also for their ability to preserve the chemical stability of extracted astaxanthin.

2. Material and methods

2.1. Material

All-*E* astaxanthin ((all-*E*)-AST, for HPLC, ≥ 97 %), L-menthol (ME, for HPLC, 99.9 %), acetic acid (C2, 99–100 %), butyric acid (C4, ≥ 99 %), hexanoic acid (C6, ≥ 99 %), octanoic acid (C8, ≥ 99 %), decanoic acid (C10, ≥ 98 %), acetone (for HPLC, 99.9 %), methanol (for HPLC, ≥ 99.9 %), acetonitrile (for HPLC, ≥ 99.9 %), ammonium acetate (for HPLC, ≥ 99 %), ethyl acetate (for HPLC, ≥ 99.8 %), sodium hydroxide (≥98 %), hydrogen chloride (37 %), ethanol (96 %), potassium persulfate (≥ 99 %), 2,2′-azinobis(3-ethylbenzothiazoline-6-sulfonic acid) diammonium salt (ABTS, 98 %), 6-hydroxy-2,5,7,8-tetramethylchroman-2-carboxylic acid (Trolox, ≥ 97 %), and 8-(diethylamino)-12H-10-oxa-5-azatetraphen-12-one (Nile Red, NR, ≥ 97 %) were purchased from Sigma-Aldrich and used as received. Food grade α-CD (CAVAMAX® W6) was kindly provided by IMCD Italy SpA (Milano, Italy). Ultra-pure water, purified by a Millipore Milli-Q system (resistivity: 18.2 MΩ cm), was used to prepare aqueous solutions.

Fresh by-products of Mediterranean red shrimp (*A. Foliacea*), composed of cephalothorax, shell, pleopods and tail, were obtained from a local seafood processing company and stored at −20 °C until use.

2.2. ME:AA mixtures preparation

Five hydrophobic binary mixtures were prepared mixing suitable amounts of each carboxylic acid (C2, C4, C6, C8, and C10) with ME. The two compounds were mixed in a round-bottom flask at 1:1 M ratio and maintained under continuous stirring at 60 °C until a liquid phase was formed. The resulting solvents (ME:C2, ME:C4, ME:C6, ME:C8 and ME:C10) were then cooled at room temperature and used for extraction experiments.

2.3. Shrimp matrix pretreatment

Frozen shrimp by-products were separated from cephalothorax and dried at 50 °C in a drying oven with fan assisted air circulation (Digitronic – Selecta) for 3–4 h. The dried shells were manually crushed by mortar and pestle and then homogenized and pulverized by a grinder (Mixer Mill MM 400, Retsch). The resulting powder, with particle size in the range 0.10–0.35 mm, was used immediately after preparation or stored at −20 °C under vacuum for subsequent uses.

2.4. Astaxanthin extraction

One-step solid/liquid extractions of AST were carried out adding a proper volume of ME:AA to a certain mass of shrimp powder to obtain

specific solid/liquid ratios. The blends were stirred by a rotating mixer for various stirring times in different experimental conditions. The samples were then centrifuged for three minutes at 500 rcf (Mikro 120 centrifuge, Hettich) and the red/orange supernatants were collected for analysis. All extraction experiments were performed in triplicate.

2.5. UV–Vis spectroscopic measurements and antioxidant capacity assessment

UV–Vis absorption measurements were conducted by means of a double beam Shimadzu UV–Vis spectrophotometer (model UV2600i/2700i). Quartz cuvettes of 1 cm pathlength were employed.

The UV–visible spectra of all ME:AA extracts were acquired in the range 350–700 nm at a resolution of 1 nm. AST concentration was assessed by the Lambert-Beer law, reading the absorbance at the peak wavelength (480 nm) and using an absorptivity of 118 ± 4 $mM^{-1}cm^{-1}$. This extinction coefficient was preliminarily determined using standard (all-*E*)-AST, as described in the Supplementary Material (Text S1 and Table S1). The influence of esterification and geometric isomerism on the AST extinction coefficient at the peak wavelength was considered negligible.

The antioxidant activity of extracts was assessed as Trolox equivalent antioxidant capacity (TEAC) using the ABTS decolorization assay, based on the scavenging activity against the colored ABTS radical [46]. Stock solutions of ABTS and potassium persulfate were mixed to obtain 7 mM and 2.45 mM concentrations respectively. The sub-stoichiometric amount of the oxidant species (persulfate) allows its complete consumption and the partial conversion of ABTS into its radical form, responsible for the dark blue-green color of the resulting solution. This stock ABTS radical solution was kept in dark at room temperature for 12–16 h before use to achieve chemical and color stability. Then, it was diluted in ethanol to reach a 0.7 absorbance value at 750 nm. All decolorization measurements were performed in time course mode according to the procedure described in a previous work [46]. Briefly, 50 μL of each standard or sample were added to 950 μL of ABTS radical solution and the profile of the absorbance drop at 750 nm was recorded for a 30 min time interval. To account for any instability of the colored species during the measurement, a suitably diluted aliquot of the ABTS radical solution was kept in the reference cuvette and the double beam mode was adopted, so that any absorbance drop could be ascribed solely to the sample (or standard) antioxidant action. Trolox standard solutions in ethanol (90, 180, 360 μM) were prepared and used as antioxidant standards to obtain the calibration curve, so that the antioxidant activity of samples was given as micromoles of Trolox equivalents per liter (TE μmol/L).

2.6. FTIR spectroscopic measurements

Mid-infrared spectra of pristine ME:AA mixtures and ME:AA extracts were acquired with a Perkin Elmer Spectrum One FTIR spectrometer equipped with a universal attenuated total reflectance (ATR) apparatus (GladiATR, Pike technologies). The internal reflection element was a single bounce diamond microprism with a diameter of 4 mm. For standard infrared absorption spectra, the background spectrum was collected with the bare microcrystal and the sample spectrum was acquired layering a drop (≈20 μL) of either pristine ME:AA or the extract onto the diamond surface. "Extract *minus* solvent" difference spectra were recorded acquiring the spectrum of the extract against a background collected on the ME:AA solvent, obtaining traces equivalent to the arithmetic difference between extract and solvent standard spectra. For standard spectra 16 interferograms were acquired and averaged, while for difference spectra 8 independent spectra of 16 interferograms each were collected and averaged, thus reaching a suitable signal to noise ratio. The resolution of all spectra was set at 4 cm^{-1}.

2.7. HPLC analysis

The chromatographic profiles of extracts were obtained by an Agilent 1100 Series HPLC System (Agilent Technologies, Palo Alto, CA) consisting of an analytical Agilent Poroshell 120 SB C18 column (2.7 μm, 150 × 4.6 mm) fitted to a binary pump (model G1312A) and a solvent degasser (model 1379A). Eluates were monitored with a 1,024-element diode array detector (model G1315B), and the system was controlled with Agilent ChemStation software for HPLC. The mobile phases were methanol–acetonitrile-water 21:16.5:62.5, vol/vol/vol containing 10 mM ammonium acetate (A) and methanol–acetonitrile-ethyl acetate 50:20:30, vol/vol/vol (B). The solvent gradient program employed was as follows: 0 min 20 % B; 0−6 min 70 % B; 6−24 min 100 % B; 24−36 min 100 % B. Flow rate was 1 mL/min. The injection volume was 10 μL. Absorbance was registered by diode array at wavelength of 480 nm. This method was adapted from the one reported by Graham and Bryant [47], allowing for faster analysis thanks to the smaller particle size. AST de-esterification was accomplished on the ethyl acetate extract by mixing 100 μL of extract with 400 μL of methanol containing 0.06 M NaOH to obtain a solution at pH 10. After dark incubation in ice for 3 h, the solution was neutralized with 100 μL of methanol containing 0.24 M HCl, dried and redissolved in 500 μL of ethyl acetate for HPLC analysis.

2.8. Emulsion preparation and characterization

For emulsion preparation, either ME:C2 or ME:C10 solvents and relevant extracts were mixed at 10 % (v/v) with an α-CD aqueous solution (0.1 g/mL). Emulsification of the mixture was accomplished using a Branson 250D digital sonifier equipped with a titanium microtip probe operating at 20 kHz frequency and set at 100 W output power, with five 2 s pulses and 2 s pauses.

To assess the stability of the incorporated AST, 2 mL emulsion aliquots were transferred in a series of test tubes, stored at room temperature in the dark, and processed at selected time intervals as follows: 4 mL of ethyl acetate were added to each tube, vortexed for 2 min and centrifuged for 2 min at 10000 rpm. The upper organic phase, containing AST, was transferred into a cuvette and the absorbance at 480 nm was measured to evaluate its concentration.

The microscopic appearance of the emulsion was assessed by confocal microscopy using Nile Red at final concentration of 5 μg/mL to stain the hydrophobic ME:AA droplets dispersed in the aqueous medium. After 5 min incubation, the sample was cast on a glass slide, covered with a coverslip and observed with a confocal microscope (LSM 5 Pascal, Carl Zeiss) using excitation wavelength of 543 nm and detection in the 560–615 nm range. Images were collected by using a 40X objective and processed with ImageJ software.

To assess the chemical composition of microdroplets dispersed in the continuous phase, the emulsion was subjected to centrifugation (500 rcf × 5 min) and the two layered phases were separated and analyzed by infrared spectroscopy.

3. Results and discussion

3.1. AST extraction efficiencies by ME:C2n (n = 1–5) mixtures

One-step solid–liquid extractions were first carried out in dark conditions at 25 °C for all ME:C2n (n = 1–5) mixtures using a solid/liquid ratio of 1/10 (g/mL). The blends were kept under continuous stirring for different extraction times (10, 20, 30 and 60 min). Afterwards, the liquid phases were separated by centrifugation and analyzed spectrophotometrically. The UV–Vis spectrum of a representative extract, specifically that one obtained with ME:C2, is shown in Fig. 1B, together with the spectrum of standard (all-*E*)-AST dissolved in the same solvent. The slight hypsochromic shift (from 486 nm to 480 nm) of the AST absorption band in the extract can be explained with the variety of AST compounds in the shrimp matrix arising from fatty acylation of hydroxyl

groups and/or *Z*-isomerism. Moreover, additional extracted compounds, absorbing at lower wavelengths, contributed to the generation of an absorption pattern not fully superimposable to that of pure (all-*E*)-AST.

Extracted AST amounts, as evaluated from visible absorption measurements and given as mass of free AST per mass of shrimp shell powder, are reported in Fig. 1C for all tested solvents as a function of incubation time. For ME:C2n (n = 2–5) solvents the extracted AST amount was constant in the investigated time interval, highlighting a fast extraction process that was completed within the first 10 min. Only in the case of ME:C2 the plateau value of extracted AST was reached after 20 min of incubation time. In agreement with a kinetically favored process, no substantial improvement of extraction efficiency was observed at higher temperatures (data not shown). Based on these results, the standard extraction conditions for subsequent measurements were set for all solvents at T = 25 °C and incubation time = 20 min. Sas et al. [48] reported a density of 0.90 g cm^{-3} at 25 °C for both ME:C8 and ME:C10, while measured viscosities were 12.54 and 15.98 mPa s respectively. Slightly higher density (0.98 g cm^{-3}) and lower viscosity (6.1 mPa s) were reported for ME:C2 although these data are relevant to a 1:2 M ratio, rather than 1:1 as in this work [49]. Hence, though higher than those of most conventional organic solvents, density and viscosity of ME:AA mixtures proved to be suitably low to favor mass transport phenomena and consequently to shorten the extraction times, in agreement with the high extraction efficiencies observed.

Overall, all five ME:AA mixtures showed comparable extraction efficiencies with an average mass of extracted AST of about 190 μg/g, a value well above most of those recently reported for a variety of shrimps species, as listed in Table 1. In the same table, the extracting solvent as well as operational conditions are also shown for each shrimp matrix. Extraction yields of biomolecules should be interpreted and compared with care since data might be affected by biomass freshness as well as by processing and dehydration conditions. Nevertheless, our data advise that *A. foliacea* can be recognized as a species highly capable of AST uptake and storage. At the same time, the hydrophobic binary mixtures here investigated proved to extract efficiently the carotenoids accumulated in *A. foliacea* shells, with operational parameters milder than those adopted in other studies, ensuring a clean, energy-saving, rapid and thus sustainable extraction process that does not require complex technologies and/or expensive reagents for the pretreatment of the solid matrix. AST extraction efficiencies from *A. foliacea* by these solvents were found comparable with those obtained by conventional solvents such as acetone (182 μg/g) and ethyl acetate (173 μg/g). Hence, ME:C2n (n = 1–5) mixtures represent a valid green alternative to these volatile, flammable and more toxic chemicals.

3.2. AST stability in ME:C2n (n = 1–5) mixtures

AST may undergo oxidation, cleavage, *E/Z* isomerization and aggregation. All these processes are modulated by specific environmental conditions, such as temperature, oxygen availability and light, and are typically accompanied by a change (both qualitative and quantitative) of the visible absorption spectrum. Hence, monitoring the time course of the absorbance of extracts at the peak wavelength (480 nm) in different environmental conditions represents a simple yet effective way for assessing the physico-chemical stability of AST pigment in all tested solvents. In our case, it is likely that oxidation and cleavage processes, rather than aggregation and isomerization, are mainly responsible for absorbance changes of ME:C10 extracts over time. The slope of a graph plotting the relative absorption intensity against time can be thus considered a measure of AST degradation rate.

In dark conditions at 25 °C (Fig. 2A) for all solvents the absorbance value at 480 nm was found to decrease with time at constant rate over a 4-day interval, thus exhibiting a pseudo zero-order kinetic profile. For longer times the absorbance change decelerated, especially in the case of ME:C2n (n = 1–4) mixtures, in agreement with concentration dependent kinetics. In ME:C10 (green plot) the extracted AST was found to degrade at the lowest rate, which was constant in all the time interval investigated. Specifically, in this solvent ≈50 % of initial peak absorbance value was retained after 11 days ensuring therefore the highest stability of dissolved AST.

Table 1
Extraction yields of AST from shrimp shell wastes achieved using different solvents and specific experimental and operational conditions, as reported in this work and in the recent literature.

Shrimp species	Solvent	Temperature (°C)	Extraction time (min)	Operational conditions	AST extraction yield (μg/g)	Reference
Aristaeomorpha foliacea (Risso, 1827)	ME:C2	25	20	mechanical stirring	199 ± 14	this study
	ME:C4				203 ± 12	
	ME:C6				199 ± 3	
	ME:C8				189 ± 2	
	ME:C10				182 ± 4	
Solenocera choprai (Nataraj, 1945)	supercritical CO_2-ethanol	50	not specified	supercritical fluid extraction	30.26 ± 0.06	[50]
not specified	ethanol 95 %	not specified	10 (for 3 times)	neutral protease pretreatment – ultrasound assisted extraction	134.20	[51]
Penaeus semisulcatus (Haan, 1844)	petroleum ether:acetone:water (15:75:10)	28	14	ultrasound assisted extraction	50.78 ± 0.15	[52]
Pandalus borealis (Krøyer, 1838)	hexane:acetone (2:3)	not specified	360	Soxhlet extraction method	187.76	[53]
	ethanol 95 %	50	20 (for 3 times)	ultrasound assisted extraction	43.7	[54]
Penaeus vannamei (Boone, 1931)	ethyl acetate	30	120	pretreatment for protein removal	101.3 ± 5.4	[55]
	ethanol and 5 % choline chloride: glycerol (1:2)	not specified	10	ultrasound assisted extraction	32.71 ± 0.72	[56]
	acetone	not specified	1	ultrasound assisted extraction	114 ± 0.4	[57]
	menthol:miristic acid (8:1)	60	120	mechanical stirring	30	[30]
Penaeus monodon (Fabricius, 1798)	choline chloride:lactic acid (1:2)	not specified	30	ultrasound assisted extraction	68.98 ± 1.22	[58]
Parapenaeus longirostris (Lucas, 1846)	ethyl esters of total fatty acids obtained from crude viscera oil	70	150	enzymatic pretreatment for protein hydrolysis	160.06 ± 8.91	[59]
	olive oil	room temperature	210	ultrasound assisted extraction	235 ± 4	[15]
not specified	L-lysine:citric acid (1:2)	40	45	acid decalcification pretreatment – ultrasound assisted extraction	112.80	[60]

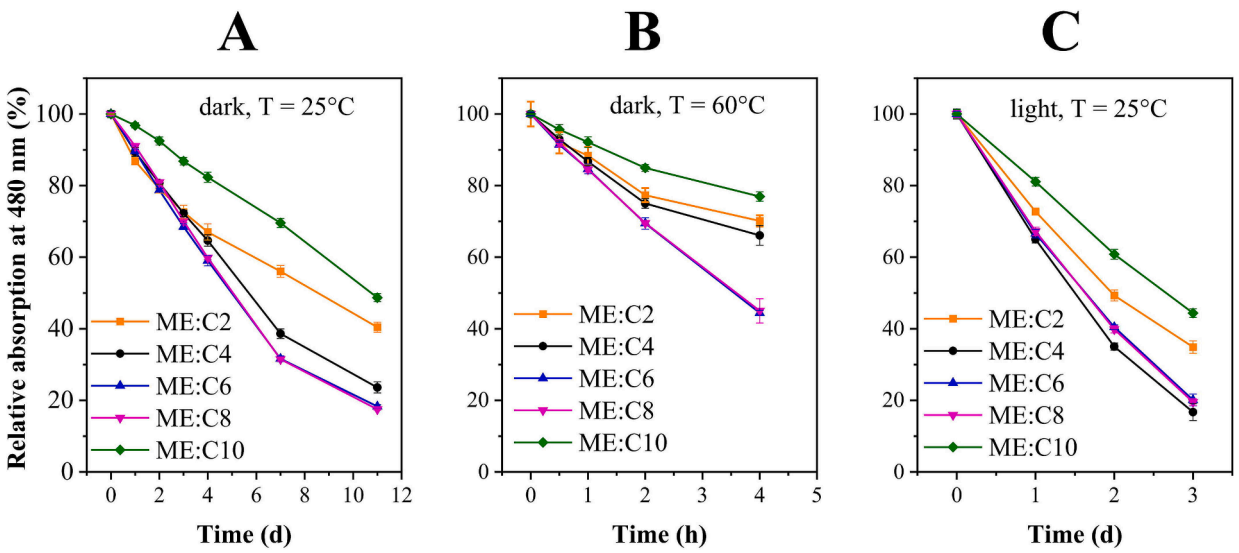

Fig. 2. **A**: Time course of the relative absorption intensity at 480 nm of the shrimp shell extracts obtained with various ME:C2n (n = 1–5) solvents kept at 25 °C in the dark. **B**: Time course of the relative absorption intensity at 480 nm of the shrimp shell extracts obtained with various ME:C2n (n = 1–5) solvents kept at 60 °C in the dark. **C**: Time course of the relative absorption intensity at 480 nm of the shrimp shell extracts obtained with various ME:C2n (n = 1–5) solvents kept in the light at 25 °C.

When the AST-rich extracts were placed in a thermostatic bath at 60 °C the pigment stability was drastically reduced in all solvents (Fig. 2B). For ME:C2 a 30-fold increase of AST degradation rate was observed in the zero-order kinetics regime, with 11 % degraded AST per hour at 60 °C against 8 % degraded AST per day at 25 °C. White light (48 W, 1800 lx) similarly favored AST physico-chemical modification, although to a minor extent (Fig. 2C). The initial rate of AST degradation increased 3 times in the case of ME:C2 (23 % degraded AST per day under illumination against 8 % per day in dark).

Comparing the results achieved, ME:C10 was found to ensure the highest stability of extracted AST in the three experimental conditions tested, followed by ME:C2.

To assess the actual performances of ME:AA mixtures with respect to conventional solvents, another set of AST degradation kinetics experiments (Supplementary Material, Fig. S1) was conducted using ME:C10 and acetone as solvents. Moreover, a pure carboxylic acid, namely C2, which is liquid at room temperature, was also tested in the same set of experiments, to assess the performances of the sole alkanoic acid component in terms of AST extraction and protection from degradation. The AST degradation kinetics profiles for acetone pointed out a much more rapid degradation of extracted AST, which was completely degraded after 8 days at 25 °C in the dark and after 2 days at the same temperature in the light. Moreover, at 60 °C in the dark, only 20 % of the original absorption of AST extracted in acetone was retained after 4 h. C2 proved to achieve good extraction yields (208 μg/g) comparable to those of ME:AA and to exert a protective effect towards extracted AST slightly lower (in dark conditions) or comparable (under light) to that one of ME:C10. This result suggests that the acidic component of the ME:AA mixtures might be responsible for the enhancement of AST stability in these solvents in line with previous investigations highlighting the protective effect of acidic pH on AST dispersed in aqueous environment [3].

Given the best performances of ME:C2 and ME:C10 in terms of AST stabilization, these two mixtures were further examined aiming to better characterize the extraction process and the extracted material.

3.3. Effect of solid–liquid ratio on AST extraction yield by ME:C2 and ME:C10

The dependence of AST extraction efficiency on the solid/liquid ratio was evaluated operating with ME:C2 and ME:C10 solvents at 25 °C and 20 min extraction time. One-step extractions were performed using the same volume (1 mL) of solvent and gradually increasing the shrimp powder mass, from 0.05 to 0.20 g, with solid/liquid ratios ranging from 1/20 to 1/5 (g/mL). Ratios higher than 1/5 could not be investigated since not adequate to guarantee the entire wetting of the solid matrix and achieve subsequent phase separation. The results, shown in Fig. 3A, highlighted for both mixtures the independence of extracted AST amounts on solid/liquid ratio, suggesting that AST concentrations in the extracts were well below the solubility limit. To confirm this hypothesis, solubility measurements were carried out with standard (all-*E*)-AST (Table 2). In ME:C2 and ME:C10 solvents the concentrations of (all-*E*)-AST in equilibrium with the solid at 25 °C were found 0.71 mM and 0.47 mM respectively, comparable to those reported for acetone and dimethyl sulfoxide [61]. These solubility values widely exceed the concentrations of AST in ME:C2 and ME:C10 shrimp shell extracts, obtained at the highest solid/liquid ratio (59 μM and 56 μM respectively). However, among the solid/liquid ratios tested, the 1/10 ratio can be considered the most suitable one, since it represents a fair compromise between solvent consumption and ease of handling in blending, centrifugation and supernatant recovery steps.

The effect of repeated extractions was also assessed, adding specific volumes of fresh solvents (either ME:C2 or ME:C10) to the shrimp shell powder resulting from the first extraction. AST amounts arising from the second-step extraction were found much lower or fully negligible, as in the case of ME:C10 (Fig. 3B), further highlighting the high efficiency of these mixtures in a single-step AST extraction process.

3.4. Chromatographic profiles of ME:C2 and ME:C10 extracts

As already discussed in paragraph 3.1, AST concentration in ME:C2 and ME:C10 extracts, assessed by visible spectrophotometry, refers to a mixture of compounds containing AST chromophores, including mono- and diesters of a variety of fatty acids. It is indeed well known that the di-alcoholic (free) form of AST in shrimp biomass represents only a minor fraction of the overall content [62]. Given the contribution of fatty acids, the actual mass of extracted AST compounds is therefore bigger than that one arising from absorbance readings and absorptivity and molar mass of free (all-*E*)-AST. Moreover, although AST occurs in shrimps mainly in the (all-*E*)-isomeric form, a certain amount of AST *Z*-isomers in

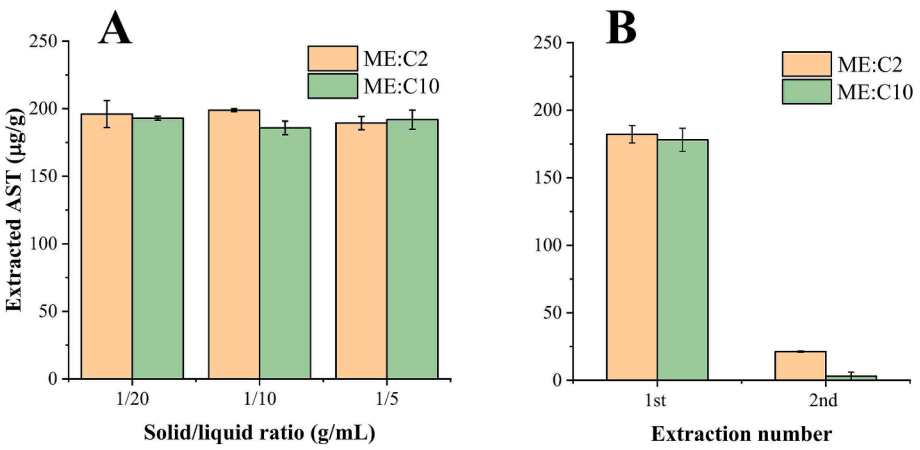

Fig. 3. **A**: Effect of the ratio between the shrimp shell powder mass and the volume of extracting solvent on the AST extraction efficiency for ME:C2 and ME:C10 solvents. **B**: AST extracted amounts arising from the first and second extraction with ME:C2 and ME:C10 solvents using the same solid/liquid ratio (1:10).

Table 2
AST concentrations in ME:C2 and ME:C10 as arising from solubility measurements at 25 °C and from extraction tests at 25 °C.

	Solvent		Solid/liquid ratio (g/mL)
	ME:C2	ME:C10	
Synthetic (all-*E*)-AST solubility at 25 °C (mM)	0.71 ± 0.03	0.47 ± 0.03	–
AST concentration in extracts (µM)	59 ± 2	56 ± 2	1:5
	30.3 ± 0.2	26.1 ± 0.8	1:10
	14.9 ± 0.8	13.6 ± 0.2	1:20

the extracts is expected [63].

To assess the relative contribution of free and esterified AST in ME:C2 and ME:C10 extracts, as well as the relative amounts of all-*E* and *Z*-isomers in the free form, the chromatographic profiles of both extracts and reference samples were recorded. As arises from Fig. 4, the chromatograms relevant to ME:C10 and ME:C2 extracts (green and orange profiles respectively) are substantially the same, indicating analogous relative concentrations of AST compounds in the two cases. According to the standard AST profile (purple), the free form of (all-*E*)-isomer presents the shortest retention time and accounts for less than 10 % of the overall xanthophyll content in ME:C2 and ME:C10 extracts. Very weak peaks at slightly higher retention times indicate negligible amounts of (9*Z*)- and (13*Z*)-isomers in the free form [64], while the subsequent numerous peaks highlight the wide variety of AST monoesters and diesters contained in the mixtures. Two main groups of signals with similar intensity patterns could be identified in the 22–27 min and 27–33 min retention time intervals, ascribable to AST monoesters and diesters respectively. Indeed, previous chromatographic profiles of shrimp extracts reported analogous main peaks [65], which were assigned to fatty acid side chains with lengths ranging between 16 and 22 carbon atoms and with up to 6 unsaturations. Alkaline hydrolysis to convert monoesters and diesters into fatty acid carboxylate salts and free AST was not feasible in the investigated mixtures due to the carboxylic acid components, which react with NaOH, thus modifying the physicochemical properties of the solvent itself and inducing AST degradation by heat release. On the other side, the conventional solvent ethyl acetate proved to extract a pool of AST compounds (black profile) quantitatively and qualitatively analogous to that obtained with ME:C10 and ME:C2. The effect of de-esterification on the chromatographic profile of *A. foliacea* shells extract was therefore assessed in this solvent (blue profile) and confirmed the assignment of peaks at high retention times to

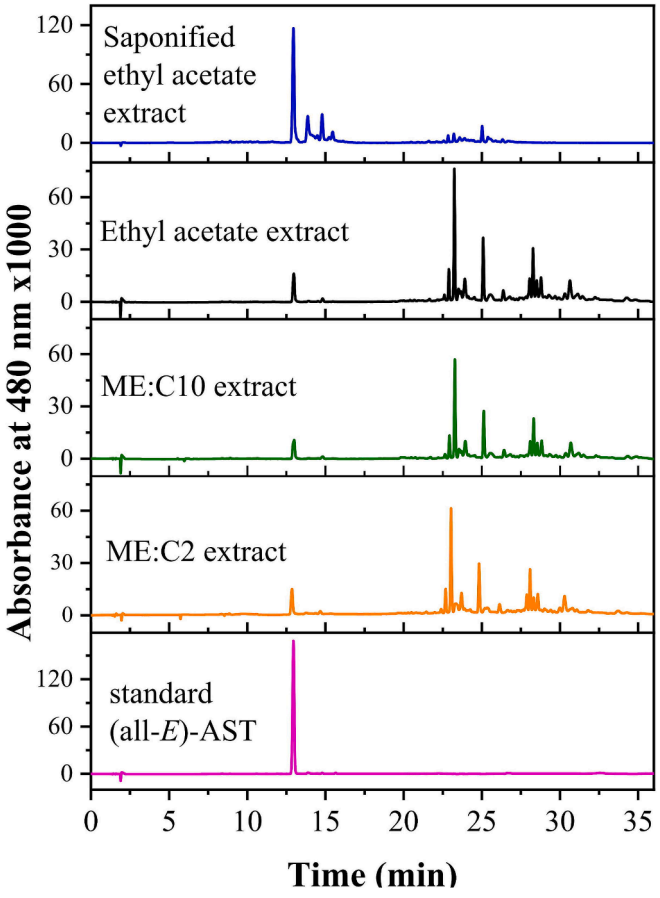

Fig. 4. Reverse phase HPLC profiles relevant to standard AST and shrimp shell extracts (see labels). AST concentrations in the injected samples were the following: 20 µM for standard (all-*E*)-AST solution, 40 µM in ME:C2 extract, 40 µM in ME:C10 extract, 45 µM in ethyl acetate extract, and 40 µM in the de-esterified ethyl acetate extract.

AST mono- and diesters. The alkaline treatment caused indeed the full disappearance of signals in the 27–33 min retention time window, due to diesters, while chromatographic peaks ascribable to monoesters were still detectable, likely due to uncomplete de-esterification of a little portion of diesters. Simultaneously, the increase of signals imputable to free AST was observed. Specifically, besides the most intense signal at 13 min retention time arising from free (all-*E*)-AST, the signals relevant

to 9*Z* and 13*Z*-isomers, at 14 and 15 min respectively, were also well evident and can be referred not only to the presence of esters of AST *Z*-isomers in the original mixture, but also to unwanted isomerization processes favored by the alkaline treatment.

3.5. Antioxidant capacity of ME:C2 and ME:C10 extracts

The antioxidant capacity of AST-rich extracts obtained with ME:C2 and ME:C10 solvents was assessed by the ABTS decolorization assay carried out in time course mode.

Vitamin E, Trolox and the so-called Trolox-like antioxidants show fast ABTS$^{\bullet}$ neutralization kinetics, resulting in square-wave decolorization profiles, while carotenoids present more complex ABTS$^{\bullet}$ neutralization kinetics, with slower but long-lasting decolorization reactions [46]. Consequently, the TEAC value of carotenoids is strictly dependent on the decolorization reading time, which is irrelevant for Trolox and Trolox-like antioxidants. The traces reported in Fig. 5A, showing the decolorization profiles for Trolox, standard (all-*E*)-AST and *A. foliacea* shrimp shells extracts, confirmed this behavior. For standard AST and extracts, the absorbance drop at 750 nm did not reach a constant value even after 30 min from sample addition. Nevertheless, at 30 min the slope of the kinetic curves was sufficiently low to ensure a good repeatability of relevant ΔA values. The decolorization extent at 30 min was thus counted for antioxidant activity assessment. The $TEAC_{30min}$ value for standard (all-*E*)-AST was found 1.3 TE mol/mol. Known this value, a prediction of $TEAC_{30min}$ of shrimp shells extracts could be done based on the AST concentration assessed spectrophotometrically. Table 3 lists experimental and predicted $TEAC_{30min}$ values of both ME:C2 and ME:C10 extracts, highlighting that their actual antioxidant capacity significantly exceeds the predicted one. This finding suggests that about 70 % of the observed antioxidant capacity is due to additional bioactive molecules co-extracted with AST, in agreement with the presence of further classes of antioxidants in shrimp biomass, such as tocopherols [12] and polyphenols [66]. Nevertheless, the occurrence of multiple forms of AST in the extracts, such as monoesters and diesters, might be partially responsible for the discrepancy among predicted and experimental TEAC values. Yang et al. [65] showed indeed that AST esters with polyunsaturated fatty acids (PUFA), exhibit higher antioxidant capacity. On the other side, Kobayashi and Sakamoto [67] demonstrated that the singlet oxygen quenching ability, assessed by a lipid photooxidation assay, was different for free and ester AST forms, depending on the hydrophobicity of the solvent employed. Therefore, the predicted antioxidant activity of extracts, based on their AST chromophore concentration and the $TEAC_{30min}$ value of free (all-*E*)-AST, represents only a rough estimate of the real contribution of AST compounds to the overall $TEAC_{30min}$ of the mixtures.

Based on these outcomes, we can conclude that ME:C2 and ME:C10 allow an efficient recovery of AST from shrimp shells, resulting in AST-rich extracts showing an antioxidant capacity superior to that of a solution containing an equivalent concentration of AST chromophores in the form of (all-*E*)-AST alone.

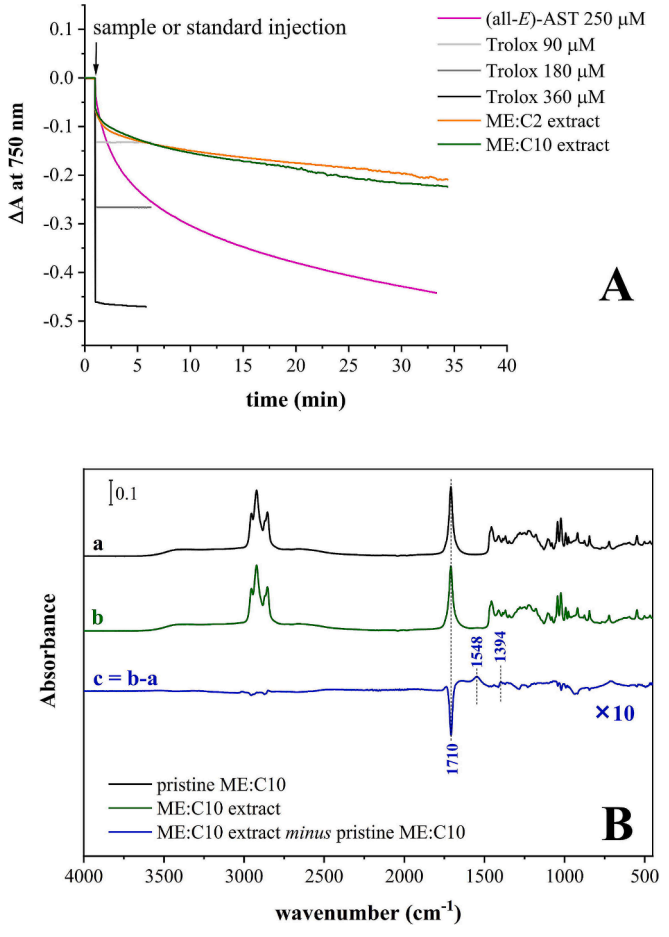

Fig. 5. A: ABTS· decolorization profiles recorded for standard antioxidant Trolox solutions in ME:C2 at various concentrations (90 µM, 180 µM and 360 µM), (all-*E*)-AST solution in ME:C2 (250 µM), ME:C2 and ME:C10 extracts from *A. foliacea* shrimp shells. **B**: ATR-FTIR spectra of ME:C10 solvent (black trace) and ME:C10 extract (green trace) from *A. foliacea* shrimp shells. The blue trace was obtained acquiring the spectrum of the extract against a background collected on the pristine ME:C10 solvent, thus being equivalent to the arithmetic difference between green and black trace. (For interpretation of the references to color in this figure legend, the reader is referred to the web version of this article.)

3.6. ATR-FTIR spectroscopy

Due to its intrinsic low sensitivity, FTIR spectroscopy is suitable to assess the major chemical components of a sample mixture, while it is usually unable to detect signals from minor constituents. This limit represents an advantage when the modification of bulk chemical composition of a complex sample has to be assessed [68]. Hence, ATR-FTIR spectroscopy was employed to verify both the capability of the binary mixtures under investigation to extract detectable (i.e. bulk) amounts of shrimp shells components, such as phospholipids, acylglycerols, peptides or polysaccharides, and the ability of the shrimp matrix to modify the intermolecular organization of the solvent.

The mid-infrared spectra of both ME:C10 solvent and its *A. foliacea* shells extract (1:10 solid/liquid ratio) are shown in Fig. 5B in black and green respectively. They exhibit the specific absorption pattern of both decanoic acid and menthol moieties, reported in Fig. S2 of the Supplementary Material), and at first glance they appear very similar to each other. Nevertheless, the difference spectrum (blue trace) highlights the selective decrease in the extract spectrum of the C=O stretching vibration at 1710 cm^{-1} (appearing as a negative band), suggesting that the interaction of ME:C10 with the shrimp shells matrix induces the deprotonation of the decanoic acid carboxylic group. The simultaneous appearance of two positive signals ascribable to antisymmetric and symmetric stretching of carboxylate at 1548 cm^{-1} and 1394 cm^{-1} further confirms the deprotonation event occurring into the mixture during the extraction process. However, the deprotonation of a

Table 3
AST concentrations and experimental and predicted $TEAC_{30min}$ values relevant to shrimp shell extracts obtained by ME:C2 and ME:C10 solvents.

Solvent	[AST] (µM)	$TEAC_{30\ min}$ (TE µmol/L)	Predicted $TEAC_{30\ min}$ (TE µmol/L)
ME:C2	36 ± 1	129 ± 6	47 ± 8
ME:C10	30 ± 1	132 ± 6	36 ± 7

carboxylic group is expected to produce an infrared absorption pattern in difference mode with a relatively more intense contribution by the carboxylate form, as reported for model carboxylic acids [69]. This finding might be explained with a role played by calcium carbonate from shrimp shells in promoting the deprotonation of some decanoic acid, with formation of calcium decanoate, which in turn partially precipitates and is removed with the pellet after the centrifugation step. The relative intensity of the negative C=O signal in the difference spectrum (Fig. 5B, blue trace) with respect to that of the C=O signal in the spectrum of ME:C10 mixture (Fig. 5B, black trace) indicates a fraction of around 7 % of decanoic acid undergoing deprotonation in the mixture. The additional weak signals detectable in the difference spectrum can be mainly ascribed to the rearrangement of menthol/decanoic acid molecules following the deprotonation-induced change of their molar ratio.

Besides this minor solvent modification, ATR-FTIR analysis allows to rule out the massive extraction of bulk shrimp shell components by ME:C10, highlighting good selectivity towards AST compounds extraction. Hydrophobic compounds coextracted with astaxanthin could be partially responsible for the weak positive bands in the difference spectrum, but the intensities observed are compatible with concentrations below 5 %. On the other hand, the contribution of extracted AST to the absorption of mid-infrared light is fully negligible due to its micromolar concentration (26.1 μM, equivalent to ≈15 ppm, see Table 2).

3.7. α-CD stabilized emulsions

Emulsions based on ME:AA mixtures have already been investigated to enhance the solubility, stability and antioxidant activity of purified carotenoids. Specifically, microemulsions composed of either ME:C2 or ME:C8 and Tween 80 aqueous solutions have been prepared and used as carriers for lutein and AST, resulting in half-life of several weeks and improved DPPH scavenging capacity with respect to organic solvents [70]. On the other hand, the use of emulsifying agents not only biocompatible and food-grade, but also possessing intrinsic health-promoting properties, is of great importance for the development of novel functional food products. In this regard, α-CD, classified as dietary fiber and hence generally recognized as safe (GRAS), can trap guest molecules within its internal cavity, with potential beneficial effects such as solubilizing and stabilizing active compounds, increasing their bioavailability and decreasing their undesirable side effects, such as masking unpleasant flavors [71]. The positive effects of α-CD on blood lipids and weight loss in both obese and nonobese healthy individuals have been recently demonstrated [72]. Interestingly, CDs are widely employed as stabilizers of oil-in-water emulsions thanks to favorable interactions of the cavity of one or more CD molecules with the oil fatty acid side chains with lengths in the range C4-C18 [73].

We therefore investigated the ability of both ME:C2 and ME:C10 to form stable ME:AA-in-water emulsions once dispersed in α-CD aqueous solutions. Emulsification was first attempted using an Ultra-Turrax

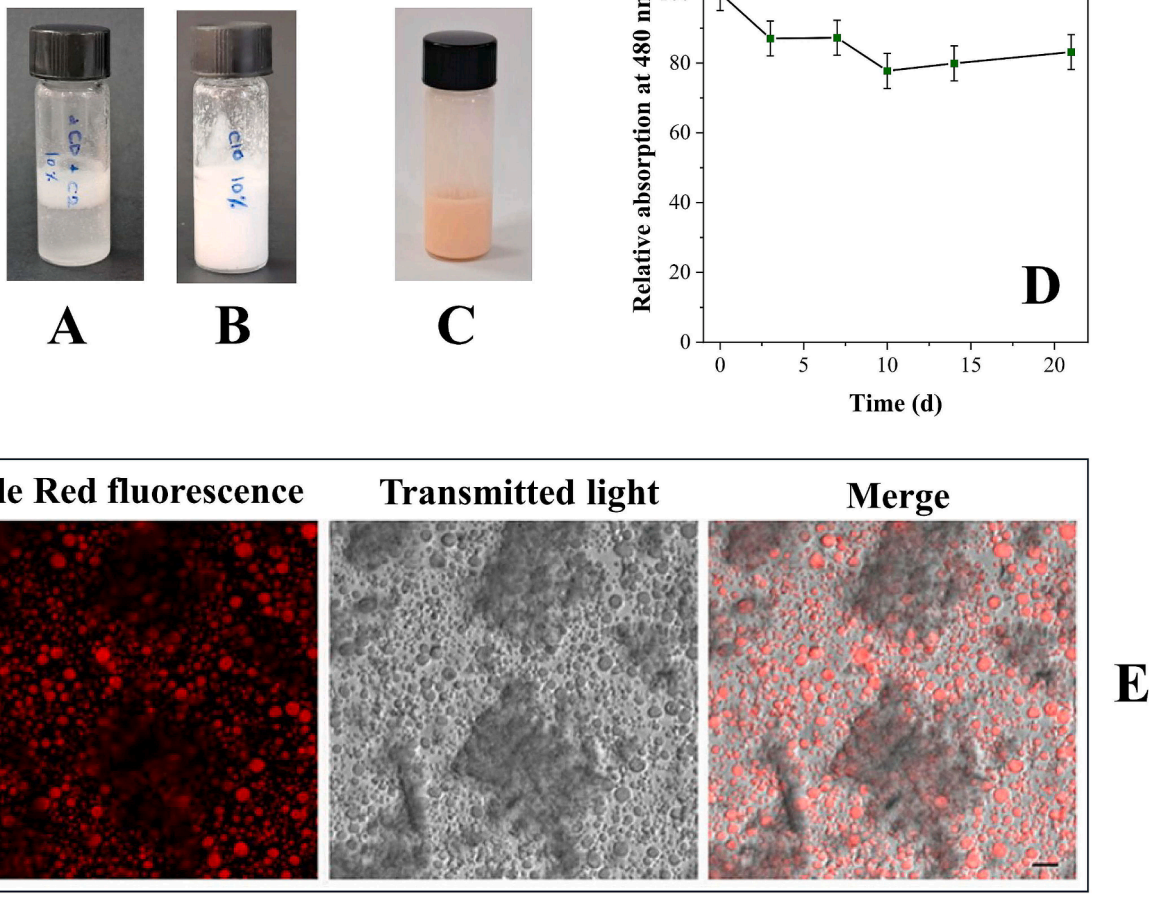

Fig. 6. A, B: Pictures of the microemulsions prepared by dispersing pristine ME:C2 (**A**) and ME:C10 (**B**) in a 0.1 g/L α-CD aqueous solution and observed after 1 h resting time. **C**: Picture of the microemulsion prepared with the *A. foliacea* shell ME:C10 extract and the α-CD aqueous solution. **D:** Time course profile of the relative absorption intensity at 480 nm of the organic phase resulting from ethyl acetate addition to the emulsion of picture **C** (see paragraph for details). **E**: Fluorescence micrographs acquired on the microemulsion of picture **C**. Nile red dye was employed to stain the hydrophobic ME:C10 phase. Scale bar = 5 μm. (For interpretation of the references to color in this figure legend, the reader is referred to the web version of this article.)

homogenizer operating at 10 k rpm for 3 min, but the dispersion process was not successful. Conversely, using a probe sonicator, as described in the experimental section, a fluid emulsion was obtained in the case of ME:C10 (Fig. 6B), which was physically stable as no sign of phase separation was observed for several days of storage at room temperature. A complete phase separation was observed instead with ME:C2 (Fig. 6A), confirming that the methyl side chain of the acetic acid is too short for effective complexation within the α-CD cavity.

The shrimp shell ME:C10 extract prepared at 1:10 solid/liquid ratio was likewise successfully emulsified with water (Fig. 6C) under the same conditions used for the pristine ME:C10. Also in this case, the dispersed system was fluid and no phase separation was observed after several days of storage in the dark at room temperature. In addition, to study the stability of the incorporated AST in the same standard conditions, the xanthophyll concentration was evaluated spectrophotometrically over time. The relevant time course profile of absorbance at 480 nm is shown in Fig. 6D, highlighting that no more than 20 % of the original AST content in the ME:C10-in-water emulsion was degraded after 21 days. As already shown in Fig. 2A, about 50 % AST degradation was instead observed in ME:C10 after 11 days, pointing out the excellent stabilization effect of the prepared emulsion.

Furthermore, the emulsion was observed by confocal microscopy to assess the shape and size of the microdomains of the eutectic mixture phase. As arises from relevant micrographs (Fig. 6E), the hydrophobic ME:C10 phase, stained with Nile Red fluorescent dye, appears distributed in spherical droplets, with an average diameter of 1.1 ± 0.3 μm, average area of 0.7 ± 0.3 μm^2 and a circularity of 0.90 ± 0.03, confirming that the dispersed system here described is indeed a ME:C10-in-water microemulsion. To investigate the composition of continuous and dispersed phases, the pristine ME:C10-in-water microemulsion was subjected to centrifugation. The resulting upper liquid was homogeneous, while the lower layer was micro-heterogeneous, presenting solid microparticles dispersed in the denser aqueous medium. Relevant ATR-FTIR spectra are shown in the Supplementary material together with reference traces of ME and C10. The spectrum of the upper phase (Fig. S2, trace c) was consistent with a ME:C10 mixture with a lower C10 content compared to the starting one (see Fig. 5B, trace b). On the other hand, the analysis of the solid material deposited on the ATR crystal after dehydration of the lower aqueous layer (Fig. S3, trace c) revealed the spectroscopic features of C10 complexed with α-CD. The formation of C10/α-CD inclusion complexes was indeed demonstrated by the strong bathochromic shift of the absorption band due to the stretching vibration of C10 C=O bonds (ν_{max} = 1558 cm^{-1}) interacting with the host α-CD. The same spectroscopic feature was observed dissolving the solid C10 in a α-CD solution (Fig. S3, trace a). The vibration of C10 carboxylic group falls at 1695 cm^{-1} in the pure solid compound (Fig. S2, trace a) and at 1694 cm^{-1} when just precipitated from an aqueous solution (Fig. S3, trace b). On the contrary, a hypsochromic shift of the same band was pointed out (ν_{max} = 1708 cm^{-1}) in the eutectic mixture (Fig. S2, trace c). No differences were observed in the C10 content of the original ME:C10 mixture when the liquid was vigorously stirred with distilled water and centrifuged (Fig. S2, trace d), highlighting the key role of α-CD in promoting C10 transfer from the eutectic mixture to the aqueous phase. These outcomes are in line with the high stability of C10/α-CD complexes, whose structure is characterized by head-to-head dimers of two cyclodextrin rings hosting the aliphatic chain of one molecule of C10, as demonstrated by crystallographic data [74]. Hence, the host–guest interaction with α-CD not only favors the transfer of C10 to the aqueous phase and the consequent menthol enrichment of the eutectic mixture, but likely plays a key role in stabilizing ME:C10 droplets in the hydrophilic environment. This finding is in line with the well-known ability of α-CD to promote the formation of Pickering emulsions [75].

4. Conclusions

The shells of *Aristaeomorpha foliacea* were identified as a rich source of AST, mainly occurring in the form of mono- and diesters. Aiming at developing a low-cost and eco-friendly process for AST recovery from this seafood industry by-product, the hydrophobic solvents composed of menthol/alkanoic acids binary mixtures proved to possess very interesting properties for efficient and fast AST extraction in mild operational conditions. The length of alkanoic acid side chain affected poorly the AST extraction efficiencies, which were in the range 182–203 μg/g, while a more pronounced influence of the side chain was observed on the stability of the extracted carotenoid. Specifically, ME:C10 guaranteed the highest chemical stability of extracted AST, followed by ME:C2. The deeper characterization of these two hydrophobic mixtures as solvents for shrimp shells outlined their excellent affinity towards xanthophylls, confirmed by synthetic (all-*E*)-AST solubility measurements (0.71 and 0.47 mM for ME:C2 and ME:C10 respectively), and their ability to co-extract additional bioactive compounds, likely responsible for antioxidant capacities, 3-fold superior to the ones predicted on the basis of the AST content. ATR-FTIR measurements, conducted in difference mode, highlighted the slight modification of the ME:C10 composition following the extraction process, mainly consisting in some loss of the alkanoic acid moiety, because of deprotonation and alkanoate precipitation. The calcium carbonate content of the shrimp shell matrix is likely responsible for this phenomenon. Unlike ME:C2, ME:C10 was found to form stable microemulsions with water using α-CD as an emulsifying agent. ME:C10-in-water emulsions were stabilized by the formation of solid microparticles of α-CD/decanoic acid inclusion complexes as revealed by infrared spectroscopy. Interestingly, these Pickering emulsions showed a strong protective effect on extracted AST, widely extending its shelf life to more than 20 days. These results encourage further investigations aimed at assessing the biocompatibility and bioactivity of AST-rich MEC10-in-water emulsions and pave the way for the development of stable formulations, suitable for applications in the field of pharmaceutics and/or cosmetics.

CRediT authorship contribution statement

Federica Mancarella: Investigation, Validation, Visualization, Methodology, Writing – original draft. **Francesco Milano:** Conceptualization, Methodology, Validation, Investigation, Visualization, Writing – original draft. **Paola Semeraro:** Conceptualization, Methodology, Writing – original draft. **Vincenzo De Leo:** Methodology, Writing – review & editing. **Francesco Messa:** Conceptualization, Resources, Methodology. **Serena Perrone:** Conceptualization, Resources, Methodology. **Antonio Salomone:** Conceptualization, Resources, Methodology, Writing – review & editing. **Miriana Durante:** Conceptualization, Methodology, Investigation, Writing – review & editing. **Marcello Salvatore Lenucci:** Conceptualization, Writing – review & editing. **Maria De Benedictis:** Investigation, Visualization. **Angelo Santino:** Supervision, Funding acquisition, Writing – review & editing. **Livia Giotta:** Conceptualization, Methodology, Validation, Visualization, Supervision, Writing – original draft, Writing – review & editing. **Ludovico Valli:** Supervision, Project administration, Funding acquisition, Writing – review & editing.

Declaration of competing interest

The authors declare that they have no known competing financial interests or personal relationships that could have appeared to influence the work reported in this paper.

Acknowledgements

This work was funded by the Italian Ministry for Universities and Research (MUR) under the “PON Ricerca e Innovazione 2014-2020”,

Action IV.4 (grant number: DOT1412034,n6) and IV.6 (grant numer: AIM1882733) and under the "National Recovery and Resilience Plan (PNRR)", Mission 4 Component 2 Investment 1.3, Theme 10 “ON Foods—Research and Innovation Network on Food and Nutrition Sustainability, Safety, and Security—Working ON Foods”.

The authors are grateful to Orazio Albano (Aquaculture and Sustainable Blue Food consultant) and Gabriella Chieffo (Entropya srl) for their support in this project.

Appendix A. Supplementary data

Supplementary data to this article can be found online at https://doi.org/10.1016/j.seppur.2025.133261.

Data availability

Data will be made available on request.

References

[1] The State of World Fisheries and Aquaculture 2022, FAO. doi: 10.4060/cc0461en.
[2] D. Coppola, C. Lauritano, F. Palma Esposito, G. Riccio, C. Rizzo, D. de Pascale, Fish waste: from problem to valuable resource, Mar. Drugs 19 (2021) 116, https://doi.org/10.3390/md19020116.
[3] G. Caruso, R. Floris, C. Serangeli, L. Di Paola, Fishery wastes as a yet undiscovered treasure from the sea: biomolecules sources, extraction methods and valorization, Mar. Drugs 18 (2020) 622, https://doi.org/10.3390/md18120622.
[4] K. Prameela, K. Venkatesh, S.B. Immandi, A.P.K. Kasturi, C.R. Krishna, C. M. Mohan, Next generation nutraceutical from shrimp waste: the convergence of applications with extraction methods, Food Chem. 237 (2017) 121–132, https://doi.org/10.1016/j.foodchem.2017.05.097.
[5] S. Gulzar, N. Raju, R.C. Nagarajarao, S. Benjakul, Oil and pigments from shrimp processing by-products: extraction, composition, bioactivities and its application-A review, Trends Food Sci. Technol. 100 (2020) 307–319, https://doi.org/10.1016/j.tifs.2020.04.005.
[6] D.E. Breithaupt, Identification and quantification of astaxanthin esters in shrimp (Pandalus borealis) and in a microalga (Haematococcus pluvialis) by liquid chromatography−mass spectrometry using negative ion atmospheric pressure chemical ionization, J. Agric. Food Chem. 52 (2004) 3870–3875, https://doi.org/10.1021/jf049780b.
[7] Z. Jia, Y. Xu, J. Wang, R. Song, Antioxidant activity and degradation kinetics of astaxanthin extracted from Penaeus sinensis (Solenocera crassicornis) byproducts under pasteurization treatment, LWT 152 (2021) 112336, https://doi.org/10.1016/j.lwt.2021.112336.
[8] N.F. Santos-Sanchez, B. Hernández-Carlos, A. Torres-Arino, R. Salas-Coronado, Astaxanthin and its formulations as potent oxidative stress inhibitors, Pharmacogn. Rev. 14 (2021) 8–15, https://doi.org/10.5530/phrev.2020.1.2.
[9] V. Rodriguez-Ruiz, J.A. Salatti-Dorado, A. Barzegari, A. Nicolas-Boluda, A. Houaoui, C. Caballo, N. Caballero-Casero, D. Sicilia, J.B. Venegas, E. Pauthe, Y. Omidi, D. Letourneur, S. Rubio, V. Gueguen, G. Pavon-Djavid, Astaxanthin-loaded nanostructured lipid carriers for preservation of antioxidant activity, Molecules 23 (2018) 2601, https://doi.org/10.3390/molecules23102601.
[10] P.A. Aneesh, K.K. Ajeeshkumar, R.G.K. Lekshmi, R. Anandan, C.N. Ravishankar, S. Mathew, Bioactivities of astaxanthin from natural sources, augmenting its biomedical potential: a review, Trends Food Sci. Technol. 125 (2022) 81–90, https://doi.org/10.1016/j.tifs.2022.05.004.
[11] Y. Kishimoto, H. Yoshida, K. Kondo, Potential anti-atherosclerotic properties of astaxanthin, Mar. Drugs 14 (2016) 35, https://doi.org/10.3390/md14020035.
[12] J. Gómez-Estaca, M.M. Calvo, I. Álvarez-Acero, P. Montero, M.C. Gómez-Guillén, Characterization and storage stability of astaxanthin esters, fatty acid profile and α-tocopherol of lipid extract from shrimp (L. vannamei) waste with potential applications as food ingredient, Food Chem. 216 (2017) 37–44, https://doi.org/10.1016/j.foodchem.2016.08.016.
[13] H. Chutia, C.L. Mahanta, Green ultrasound and microwave extraction of carotenoids from passion fruit peel using vegetable oils as a solvent: optimization, comparison, kinetics, and thermodynamic studies, IFSET 67 (2021) 102547, https://doi.org/10.1016/j.ifset.2020.102547.
[14] J. Pu, P.J. Bechtel, S. Sathivel, Extraction of shrimp astaxanthin with flaxseed oil: effects on lipid oxidation and astaxanthin degradation rates, Biosyst. Eng. 107 (2010) 364–371, https://doi.org/10.1016/j.biosystemseng.2010.10.001.
[15] I. Panagiotakopoulos, H.C. Karantonis, I.G. Kartelias, C. Nasopoulou, Ultrasonic-assisted extraction of astaxanthin from shrimp by-products using vegetable oils, Mar. Drugs 21 (2023) 467, https://doi.org/10.3390/md21090467.
[16] E. Yara-Varón, Y. Li, M. Balcells, R. Canela-Garayoa, A.-S. Fabiano-Tixier, F. Chemat, Vegetable oils as alternative solvents for green oleo-extraction, purification and formulation of food and natural products, Molecules 22 (2017) 1474, https://doi.org/10.3390/molecules22091474.
[17] C. Hemanta Chutia, C.L. Mahanta, Green ultrasound and microwave extraction of carotenoids from passion fruit peel using vegetable oils as a solvent: optimization, comparison, kinetics, and thermodynamic studies, Innov. Food Sci. Emerg. Technol. 67 (2021) 102547, https://doi.org/10.1016/j.ifset.2020.102547.
[18] A.P. Abbott, D. Boothby, G. Capper, D.L. Davies, R.K. Rasheed, Deep eutectic solvents formed between choline chloride and carboxylic acids: versatile alternatives to ionic liquids, J. Am. Chem. Soc. 126 (2004) 9142–9147, https://doi.org/10.1021/ja048266j.
[19] C. McReynolds, A. Adrien, N. Castejon, S.C.M. Fernandes, Green in the deep blue: deep eutectic solvents as versatile systems for the processing of marine biomass, GCLR 15 (2022) 383–404, https://doi.org/10.1080/17518253.2022.2065890.
[20] B.B. Hansen, S. Spittle, B. Chen, D. Poe, Y. Zhang, J.M. Klein, A. Horton, L. Adhikari, T. Zelovich, B.W. Doherty, B. Gurkan, E.J. Maginn, A. Ragauskas, M. Dadmun, T.A. Zawodzinski, G.A. Baker, M.E. Tuckerman, R.F. Savinell, J. R. Sangoro, Deep eutectic solvents: a review of fundamentals and applications, Chem. Rev. 121 (2021) 1232–1285, https://doi.org/10.1021/acs.chemrev.0c00385.
[21] M.A.R. Martins, S.P. Pinho, J.A.P. Coutinho, Insights into the nature of eutectic and deep eutectic mixtures, J Solution Chem 48 (2019) 962–982, https://doi.org/10.1007/s10953-018-0793-1.
[22] E.L. Smith, A.P. Abbott, K.S. Ryder, Deep eutectic solvents (DESs) and their applications, Chem. Rev. 114 (2014) 11060–11082, https://doi.org/10.1021/cr300162p.
[23] D.O. Abranches, M.A.R. Martins, L.P. Silva, N. Schaeffer, S.P. Pinho, J.A. P. Coutinho, Phenolic hydrogen bond donors in the formation of non-ionic deep eutectic solvents: the quest for type V DES, Chem. Commun. 55 (2019) 10253–10256, https://doi.org/10.1039/C9CC04846D.
[24] B.D. Ribeiro, C. Florindo, L.C. Iff, M.A.Z. Coelho, I.M. Marrucho, Menthol-based eutectic mixtures: hydrophobic low viscosity solvents, ACS Sustain. Chem. Eng. 3 (2015) 2469–2477, https://doi.org/10.1021/acssuschemeng.5b00532.
[25] M.A.R. Martins, E.A. Crespo, P.V.A. Pontes, L.P. Silva, M. Bülow, G.J. Maximo, E.A. C. Batista, C. Held, S.P. Pinho, J.A.P. Coutinho, Tunable hydrophobic eutectic solvents based on terpenes and monocarboxylic acids, ACS Sustain. Chem. Eng. 6 (2018) 8836–8846, https://doi.org/10.1021/acssuschemeng.8b01203.
[26] T. Křížek, M. Bursová, R. Horsley, M. Kuchař, P. Tůma, R. Čabala, T. Hložek, Menthol-based hydrophobic deep eutectic solvents: towards greener and efficient extraction of phytocannabinoids, J. Clean. Prod. 193 (2018) 391–396, https://doi.org/10.1016/j.jclepro.2018.05.080.
[27] H. Shaaban, Sustainable dispersive liquid–liquid microextraction method utilizing a natural deep eutectic solvent for determination of chloramphenicol in honey: assessment of the environmental impact of the developed method, RSC Adv., 13 (2023) 5058–5069, https://doi.org/10.1039/D2RA08221G.
[28] N. Paul, G. Harish, T. Banerjee, Stability mechanism of menthol and fatty acid based hydrophobic eutectic solvents: insights from nonbonded interactions, ACS Sustain. Chem. Eng. 8 (2023) 3539–3556, https://doi.org/10.1021/acssuschemeng.2c06137.
[29] O.G. Sas, L. Villar, Á. Domínguez, B. González, E.A. Macedo, Hydrophobic deep eutectic solvents as extraction agents of nitrophenolic pollutants from aqueous systems, Environ. Technol. Innov. 25 (2022) 102170, https://doi.org/10.1016/j.eti.2021.102170.
[30] L.A. Rodrigues, C.V. Pereira, I.C. Leonardo, N. Fernández, F.B. Gaspar, J.M. Silva, R.L. Reis, A.R.C. Duarte, A. Paiva, A.A. Matias, Terpene-based natural deep eutectic systems as efficient solvents to recover astaxanthin from brown crab shell residues, ACS Sust. Chem. Eng. 8 (2020) 2246–2259, https://doi.org/10.1021/acssuschemeng.9b06283.
[31] M. Díaz-Álvarez, A. Martín-Esteban, Preparation and further evaluation of l-menthol-based natural deep eutectic solvents as supported liquid membrane for the hollow fiber liquid-phase microextraction of sulfonamides from environmental waters, Adv. Sample Prep. 4 (2022) 100047, https://doi.org/10.1016/j.sampre.2022.100047.
[32] A.G. Pekel, E. Kurtulbaş, I. Toprakçı, S. Sahin, Menthol-based deep eutectic solvent for the separation of carbamazepine: reactive liquid-liquid extraction, Biomass Conv. Bioref. 12 (2022) 1249–1256, https://doi.org/10.1007/s13399-020-00707-z.
[33] C. Florindo, L.C. Branco, I.M. Marrucho, Quest for green-solvent design: from hydrophilic to hydrophobic (Deep) eutectic solvents, Chem Sus. Chem 12 (2019) 1549–1559, https://doi.org/10.1002/cssc.201900147.
[34] F. Villalobos-Castillejos, P. Cerezal-Mezquita, M.L. Hernández-De Jesús, B. E. Barragán-Huerta, Production and stability of water-dispersible astaxanthin oleoresin from Phaffia rhodozyma, Int. J. Food Sci. Technol. 48 (2013) 1243–1251, https://doi.org/10.1111/ijfs.12083.
[35] S. Della Posta, V. Gallo, A. Gentili, C. Fanali, Strategies for the recovery of bioactive molecules from deep eutectic solvents extracts, Trends Anal. Chem. 157 (2022) 116798, https://doi.org/10.1016/j.trac.2022.116798.
[36] M. Devi, R. Moral, S. Thakuria, A. Mitra, S. Paul, Hydrophobic deep eutectic solvents as greener substitutes for conventional extraction media: examples and techniques, ACS Omega 8 (2023) 9702–9728, https://doi.org/10.1021/acsomega.2c07684.
[37] C. Ferreira, M. Sarraguça, A comprehensive review on deep eutectic solvents and its use to extract bioactive compounds of pharmaceutical interest, Pharmaceuticals 17 (2024) 124, https://doi.org/10.3390/ph17010124.
[38] G.P.P. Kamatou, I. Vermaak, A.M. Viljoen, B.M. Lawrence, Menthol: a simple monoterpene with remarkable biological properties, Phytochem. 96 (2013) 15–25, https://doi.org/10.1016/j.phytochem.2013.08.005.
[39] C.B. Huang, Y. Altimova, T.M. Myers, J.L. Ebersole, Short- and medium-chain fatty acids exhibit antimicrobial activity for oral microorganisms, Arch. Oral Biol. 2011 (56) (2012) 650–654, https://doi.org/10.1016/j.archoralbio.2011.01.011.

[40] P.G. Roopashree, S.S. Shetty, N.S. Kumari, Effect of medium chain fatty acid in human health and disease, J. Funct. Foods 87 (2021) 104724, https://doi.org/10.1016/j.jff.2021.104724.
[41] P. Semeraro, G. Chimienti, E. Altamura, P. Fini, V. Rizzi, P. Cosma, Chlorophyll a in cyclodextrin supramolecular complexes as a natural photosensitizer for photodynamic therapy (PDT) applications, Mater. Sci. Eng. C 85 (2018) 47–56, https://doi.org/10.1016/j.msec.2017.12.012.
[42] V. Rizzi, S. Matera, P. Semeraro, P. Fini, P. Cosma, Interactions between 4-thiothymidine and water-soluble cyclodextrins: evidence for supramolecular structures in aqueous solutions, Beilstein J. Org. Chem. 12 (2016) 549–563, https://doi.org/10.3762/bjoc.12.54.
[43] B.G. Mathapa, V.N. Paunov, Cyclodextrin stabilised emulsions and cyclodextrinosomes, Phys. Chem. Chem. Phys. 15 (2013) 17903–17914, https://doi.org/10.1039/C3CP52116H.
[44] M. Durante, F. Milano, M.D. Caroli, L. Giotta, G. Piro, G. Mita, M. Frigione, M. S. Lenucci, Tomato oil encapsulation by α-, β-, and γ-cyclodextrins: a comparative study on the formation of supramolecular structures, antioxidant activity, and carotenoid stability, Foods 9 (2020) 1553, https://doi.org/10.3390/foods9111553.
[45] G. Balenzano, G.F. Racaniello, I. Arduino, A.A. Lopedota, A. Lopalco, V. Laquintana, N. Denora, Cyclodextrin-based supramolecular deep eutectic solvent (CycloDES): a vehicle for the delivery of poorly soluble drugs, Int. J. Pharm. 647 (2023) 123553, https://doi.org/10.1016/j.ijpharm.2023.123553.
[46] D. Mastrogiacomo, M.S. Lenucci, V. Bonfrate, M. Di Carolo, G. Piro, L. Valli, L. Rescio, F. Milano, R. Comparelli, V. De Leo, L. Giotta, Lipid/detergent mixed micelles as a tool for transferring antioxidant power from hydrophobic natural extracts into bio-deliverable liposome carriers: the case of lycopene rich oleoresins, RSC Adv. 5 (2015) 3081–3093, https://doi.org/10.1039/C4RA12254B.
[47] J.E. Graham, D.A. Bryant, The biosynthetic pathway for synechoxanthin, an aromatic carotenoid synthesized by the euryhaline, unicellular cyanobacterium Synechococcus sp. Strain PCC 7002, J. Bacteriol. 190 (2008) 7966–7974, https://doi.org/10.1128/jb.00985-08.
[48] O.G. Sas, M. Castro, Á. Domínguez, B. González, Removing phenolic pollutants using Deep Eutectic Solvents, Sep. Purif. Technol. 227 (2019) 115703, https://doi.org/10.1016/j.seppur.2019.115703.
[49] J. Cao, E. Su, Hydrophobic deep eutectic solvents: the new generation of green solvents for diversified and colorful applications in green chemistry, J. Clean. Prod. 314 (2021) 127965, https://doi.org/10.1016/j.jclepro.2021.127965.
[50] P.A. Aneesh, R. Anandan, L.R.G. Kumar, K.K. Ajeeshkumar, K.A. Kumar, S. Mathew, A step to shell biorefinery—Extraction of astaxanthin-rich oil, protein, chitin, and chitosan from shrimp processing waste, Biomass Conv. Bioref. 13 (2023) 205–214, https://doi.org/10.1007/s13399-020-01074-5.
[51] L. Wang, J. Hu, W. Lv, W. Lu, D. Pei, Y. Lv, W. Wang, M. Zhang, R. Ding, M. Lv, Optimized extraction of astaxanthin from shrimp shells treated by biological enzyme and its separation and purification using macroporous resin, Food Chem. 363 (2021) 130369, https://doi.org/10.1016/j.foodchem.2021.130369.
[52] P. Sharayei, E. Azarpazhooh, S. Zomorodi, S. Einafshar, H.S. Ramaswamy, Optimization of ultrasonic-assisted extraction of astaxanthin from green tiger (Penaeus semisulcatus) shrimp shell, Ultrason. Sonochem. 76 (2021) 105666, https://doi.org/10.1016/j.ultsonch.2021.105666.
[53] I. Phadtare, H. Vaidya, K. Hawboldt, S.K. Cheema, Shrimp oil extracted from shrimp processing by-product is a rich source of omega-3 fatty acids and astaxanthin-esters, and reveals potential anti-adipogenic effects in 3T3-L1 adipocytes, Mar. Drugs 19 (2021) 259, https://doi.org/10.3390/md19050259.
[54] J. Hu, W. Lu, M. Lv, Y. Wang, R. Ding, L. Wang, Extraction and purification of astaxanthin from shrimp shells and the effects of different treatments on its content, Rev. Bras 29 (2019) 24–29, https://doi.org/10.1016/j.bjp.2018.11.004.
[55] J.-J. Deng, H.-H. Mao, W. Fang, Z.-Q. Li, D. Shi, Z.-W. Li, T. Zhou, X.-C. Luo, Enzymatic conversion and recovery of protein, chitin, and astaxanthin from shrimp shell waste, J. Clean. Prod. 271 (2020) 122655, https://doi.org/10.1016/j.jclepro.2020.122655.
[56] C. Dos Santos, C. Padilha, K. Damasceno, P. Leite, A. De Araújo, P. Freitas, E. Vieira, A. Cordeiro, F. De Sousa Jr, C. De Assis, Astaxanthin recovery from shrimp residue by solvent ethanol extraction using choline chloride:glycerol deep eutectic solvent as adjuvant, J. Braz. Chem. Soc. (2021), https://doi.org/10.21577/0103-5053.20210005.
[57] J.M. Montoya, S.V. Mata, J.L. Acosta, B. Edgar, H. Cabrera, L.G.L. Valdez, C. Reyes, H. Jair, B. Cureño, Obtaining of astaxanthin from crab exosqueletons and shrimp head shells, Bioint. Res. Appl. Chem. 11 (2021) 13516–13523, https://doi.org/10.33263/BRIAC 115.1351613523.
[58] V. Chandra Roy, T.C. Ho, H.-J. Lee, J.-S. Park, S.Y. Nam, H. Lee, A.T. Getachew, B.-S. Chun, Extraction of astaxanthin using ultrasound-assisted natural deep eutectic solvents from shrimp wastes and its application in bioactive films, J. Clean. Prod. 284 (2021) 125417, https://doi.org/10.1016/j.jclepro.2020.125417.
[59] C.M. Messina, S. Manuguerra, R. Arena, G. Renda, G. Ficano, M. Randazzo, S. Fricano, S. Sadok, A. Santulli, In vitro bioactivity of astaxanthin and peptides from hydrolisates of shrimp (Parapenaeus longirostris) by-products: from the extraction process to biological effect evaluation, as pilot actions for the strategy "from waste to profit.", Mar. Drugs 19 (2021) 216, https://doi.org/10.3390/md19040216.
[60] M. Denga, Y. Qu, T. Wu, Y. Na, N. Liang, L. Zhao, Amino acid-based natural deep eutectic solvent combined with ultrasonic extraction: green extraction of astaxanthin from shrimp shells, Biomass Conv. Bioref. (2023), https://doi.org/10.1007/s13399-023-04660-5.
[61] A. Gherabli, N. Grimi, J. Lemaire, E. Verobiev, N. Lebovka, Extraction of valuable biomolecules from the microalga Haematococcus pluvialis assisted by electrotechnologies, Molecules 28 (2023) 2089, https://doi.org/10.3390/molecules28052089.
[62] J.A. Núñez-Gastélum, D.I. Sánchez-Machado, J. López-Cervantes, J.R. Rodríguez-Núñez, M.A. Correa-Murrieta, R.G. Sánchez-Duarte, O.N. Campas-Baypoli, Astaxanthin and its esters in pigmented oil from fermented shrimp by-products, J. Aquat. Food Prod. Technol. 25 (2016) 334–343, https://doi.org/10.1080/10498850.2013.851756.
[63] W. Yu, J. Liu, Astaxanthin isomers: selective distribution and isomerization in aquatic animals, Aquaculture 520 (2020) 734915, https://doi.org/10.1016/j.aquaculture.2019.734915.
[64] C. Yang, L. Zhang, H. Zhang, Q. Sun, R. Liu, J. Li, L. Wu, R. Tsao, Rapid and efficient conversion of all-E-astaxanthin to 9Z- and 13Z-Isomers and assessment of their stability and antioxidant activities, J. Agric. Food Chem. 65 (2017) 818–826, https://doi.org/10.1021/acs.jafc.6b04962.
[65] L. Yang, X. Qiao, J. Liu, L. Wu, Y. Cao, J. Xu, C. Xue, Preparation, characterization and antioxidant activity of astaxanthin esters with different molecular structures, J Sci Food Agric 101 (2021) 2576–2583, https://doi.org/10.1002/jsfa.10887.
[66] A.C. Onodenalore, A. Hossain, J. Banoub, F. Shahidi, Unique heterocyclic phenolic compounds from shrimp (Pandalus borealis) and beyond, Food Prod Process and Nutr 6 (2024) 29, https://doi.org/10.1186/s43014-023-00215-3.
[67] M. Kobayashi, Y. Sakamoto, Singlet oxygen quenching ability of astaxanthin esters from the green alga Haematococcus pluvialis, Biotechnol. Lett. 21 (1999) 265–269, https://doi.org/10.1023/A:1005445927433.
[68] P. Semeraro, L. Giotta, A. Talà, M. Tufariello, M. D'Elia, F. Milano, P. Alifano, L. Valli, A simple strategy based on ATR-FTIR difference spectroscopy to monitor substrate intake and metabolite release by growing bacteria, Spectrochim. Acta - a: Mol. Biomol. Spectrosc. 302 (2023) 123031, https://doi.org/10.1016/j.saa.2023.123031.
[69] L. Giotta, D. Mastrogiacomo, F. Italiano, F. Milano, A. Agostiano, K. Nagy, L. Valli, M. Trotta, Reversible binding of metal ions onto bacterial layers revealed by protonation-induced ATR-FTIR difference spectroscopy, Langmuir 27 (2011) 3762–3773, https://doi.org/10.1021/la104868m.
[70] Y. Li, K. Hu, C. Huang, Y. Hu, H. Ji, S. Liu, J. Gao, Improvement of solubility, stability and antioxidant activity of carotenoids using deep eutectic solvent-based microemulsions, Colloids Surf. b: Biointerfaces 217 (2022) 112591, https://doi.org/10.1016/j.colsurfb.2022.112591.
[71] A. Gonzalez Pereira, M. Carpena, P. García Oliveira, J.C. Mejuto, M.A. Prieto, J. Simal Gandara, Main applications of cyclodextrins in the food industry as the compounds of choice to form host–guest complexes, Int. J. Mol. Sci. 22 (2021), https://doi.org/10.3390/ijms22031339.
[72] K.B. Comerford, J.D. Artiss, K.L.C. Jen, S.E. Karakas, The beneficial effects of α-cyclodextrin on blood lipids and weight loss in healthy humans, Obesity (Silver Spring) 19 (2011) 1200–1204, https://doi.org/10.1038/oby.2010.280.
[73] D. Duchêne, A. Bochot, S.-C. Yu, C. Pépin, M. Seiller, Cyclodextrins and emulsions, Int. J. Pharm. 266 (2003) 85–90, https://doi.org/10.1016/S0378-5173(03)00384-3.
[74] S. Rodríquez-Llamazares, N. Yutronic, P. Jara, U. Englert, M. Noyong, U. Simon, The structure of the first supramolecular α-cyclodextrin complex with an aliphatic monofunctional carboxylic acid, Eur. J. Org. Chem., 4298–4300 (2007), https://doi.org/10.1002/ejoc.200700454.
[75] R. Diaz-Salmeron, I. Chaab, F. Carn, M. Djabourov, K. Bouchemal, Pickering emulsions with α-cyclodextrin inclusions: structure and thermal stability, J. Colloid Interface Sci., 482 (2016) 48–57, https://doi.org/10.1016/j.jcis.2016.07.033.